Journal of Magnetic Resonance **142,** 294–299 (2000)
doi:10.1006/jmre.1999.1939, available online at http://www.idealibrary.com on IDEAL®

Sensitivity Improvement and New Acquisition Scheme of Heteronuclear Active-Coupling-Pattern-Tilting Spectroscopy

Wiktor Koźmiński* and Daniel Nanz†

**Department of Chemistry, Warsaw University, ul. Pasteura 1, 02-093 Warsaw, Poland; and †Universitätsspital Zürich, Departement Medizinische Radiologie, Magnetresonanz-Zentrum, Rämistrasse 100, CH-8091 Zürich, Switzerland*

Received June 16, 1999; revised September 13, 1999

A simplified phase-cycling scheme for heteronuclear active-coupling-pattern tilting (ACT) spectroscopy is presented. It is demonstrated that the theoretically expected twofold sensitivity gain over earlier implementations can be experimentally realized. A further intensity increase by a factor of 2 is obtained with standard sensitivity-enhancement pulse-sequence elements. The HSQC–HECADE sequence presented is designed for an accurate determination of heteronuclear one-bond and, with subsequent I-spin isotropic mixing, long-range coupling constants. As an exemplary application, the determination of the $^3J_{N,H\beta}$ coupling constants in a peptide at natural isotope abundance is demonstrated. Additionally, a new polarization-transfer step for the long-range HSQC–HECADE experiment is proposed which avoids a fixed delay tuned to a specific coupling-constant value. Thus, the long-range correlation experiment does not require prior knowledge of the coupling constants to be measured and yields more uniform cross-peak intensity for a broad range of active coupling constants.

Key Words: J-**couplings; active-coupling-pattern tilting; ACT; accordion spectroscopy; HSQC, sensitivity enhancement.**

INTRODUCTION

Previously, we proposed HMQC- and HSQC-based 2D NMR experiments (HECADE) for the determination of heteronuclear coupling constants (*1*) that—in contrast to E. COSY—yield tilted cross-peak patterns even for two-spin systems and thus accurate values of active coupling constants. The values of passive and long-range coupling constants can be obtained through the addition of I-spin magnetization-transfer steps into the pulse sequence. The tilt of the multiplet patterns results from an appropriate coaddition of in- and antiphase coherences along the two dimensions of the 2D spectra. In a further expansion of the basic idea to pure-phase homo- and heteronuclear *J* spectroscopy it was referred to as active-coupling-pattern tilting (ACT) (*2*). The main drawback of the early ACT implementations was their complicated basic four-step phase cycle. In the first two scans pure in-phase and in the next two pure antiphase signals were acquired and added together with suitable $\pi/2$ phase shifts in both dimensions. The second half of the useful signal, antiphase and in-phase in the first and second pair of scans, respectively, was canceled and consequently lost while obtaining the appropriate cross-peak tilts. However, as was demonstrated in the next application to broadband homonuclear decoupled homonuclear correlation spectroscopy (ACT-ct-COSY) (*3*), it is possible to obtain a twofold sensitivity gain by a simplification of the phase cycle and the corresponding data-processing scheme applied. An additional sign inversion of the antiphase coherences in either echo- or, for complementary tilting, in antiecho experiments is necessary in the case of experiments with an echo–antiecho coherence selection by pulsed field gradients (PFG). Apart from the improved signal to noise ratio this modification significantly simplifies the actual pulse-sequence coding on commercial spectrometers. Additionally, the fourfold shortening of the basic phase cycle allows spectra acquisitions with only one scan per single FID as long as the signal is large enough. Alternatively, extended phase cycling for a cleaner coherence-pathway selection is possible when more scans are necessary. Although we previously reported HECADE sequences based on HMQC as well as on HSQC experiments (*1*) we will focus here on the latter. Being shorter, they should have an advantage in applications to molecules with short T_2.

RESULTS AND DISSCUSION

The pulse-sequence scheme for the improved HSQC–HECADE experiments with one-bond polarization transfer is depicted in Fig. 1. The presented sequence is derived from the standard (*4*) and sensitivity enhanced (*5*) PFG versions of the HSQC experiment followed by a t_1^* period for $^1J_{IS}$ evolution, which is incremented synchronously with t_1. The t_1^*/t_1 ratio determines the apparent $^1J_{IS}$ splitting in the F_1 domain which can be optimized at will within the limits set by T_2 relaxation. The sensitivity enhancement and an I-spin isotropic mixing are optional, however, for the measurement of long-range IS coupling constants the additional I-spin transfer is necessary. I-spin homonuclear-coupling and chemical-shift evolution are refocused in the center of the t_1^* period by an element R which, e.g., represents a BIRDx pulse (*6, 7*) (Fig. 1b) or, alternatively, a spectral-region selective π-pulse (Fig. 1c). In the case of $^1H,^{15}N$ experiments with peptides, the second possibility is preferred because H_N-proton-region selective refocusing pulses

1090-7807/00 $35.00

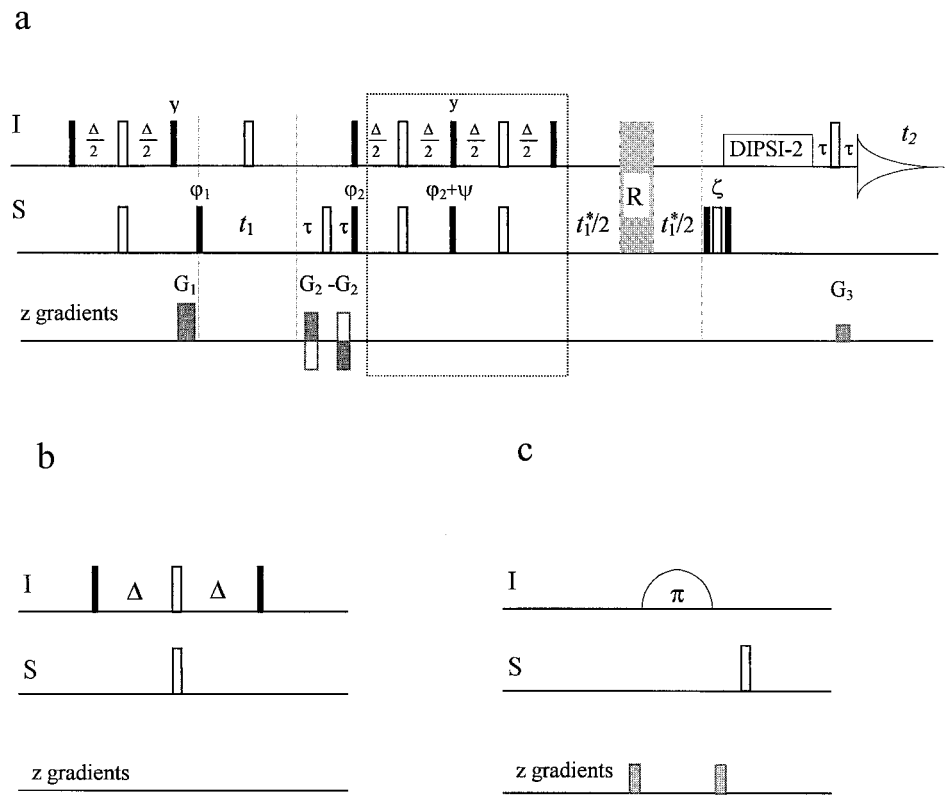

FIG. 1. (a) Pulse sequence of the HSQC–HECADE experiment. Dark-filled and open bars represent $\pi/2$ and π pulses, respectively. All pulses are applied along the rotating-frame x axis unless indicated differently. The delay Δ should be tuned to $0.5/^1J_{IS}$. τ includes the rectangular-shape gradient pulse and a 100-μs recovery time. Gradient G_1 was applied with an amplitude of 10 G/cm and a duration of 2 ms. Gradients G_2 and G_3 with a duration of 2.5 and 1 ms, and an amplitude of ± 10 and 5 G/cm, respectively, were used for echo–antiecho selection, depending on the sign of G_2. Additionally, the sign of the antiphase coherences is reversed by a $\pi/2$ phase shift of ζ in the antiecho experiment at each t_1. The basic phase cycle was $\varphi_1 = x, -x, \varphi_2 = x, x, -x, -x, \zeta = -x$, and receiver $x, -x, -x, x$. The sensitivity-enhancement scheme requires phase ψ to be set to $-\pi/2$ in echo, and $\pi/2$ in antiecho experiments, respectively. Data combination and processing was done with standard VNMR software. Two refocusing elements R at the center of the t_1^* period are suggested, (b) a BIRDx and (c) spectral-region selective $(\pi)_I$ pulse, optionally flanked with gradients, followed by a hard $(\pi)_S$ pulse. In the present work, both possibilities were tested. However, in case of fast transverse relaxation the shorter version is to be preferred. The sensitivity-enhancement pulse-sequence elements in the dotted box are optional.

can be significantly shorter than a corresponding BIRD pulse. As in the original application, a sign inversion of the antiphase coherences in successive echo and antiecho experiments is obtained by a composite 0 or π S-spin pulse, respectively, at the end of the t_1^* period. At the expense of unequal lengths of echo and antiecho experiments the composite 0 pulse could also be omitted. The data are processed by standard echo–antiecho 2D Fourier transformation procedures. When the sensitivity enhancement is not applied tilted lines in antiphase are obtained (Scheme 1a), whereas with sensitivity enhancement in-phase tilted signals with twofold sensitivity improvement for the IS spin systems are observed (Scheme 1b). Although the tilt of one-bond correlation peaks does not depend on the sign of the coupling constant, the sign of the relative tilt of the two doublet components indicates the relative signs of the corresponding $^1J_{IS}$ and $^nJ_{IS}$ coupling constants for multiple bond cross peaks.

The improvement of the obtainable signal to noise ratio in comparison with the previously published HECADE implementation is illustrated in Fig. 2. The relative signal intensities in these ^{1}H, ^{15}N experiments at natural isotope abundance are very close to the expected theoretical values. Figures 3 and 4 display H_N and H_β regions of ^{1}H,^{15}N spectra obtained with

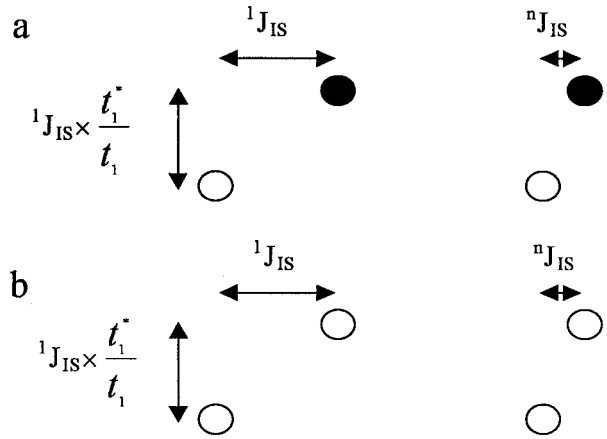

SCHEME 1

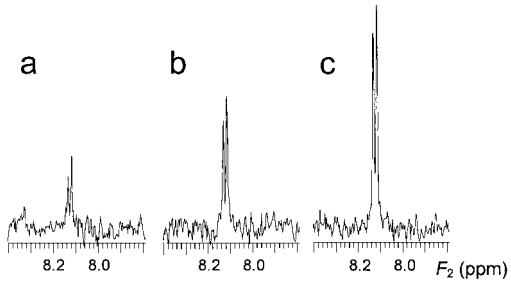

FIG. 2. Comparison of F_2-trace intensities of the upfield doublet component of the Asn5 NH cross-peak in ^1H,^{15}N-HSQC–HECADE spectra of the [Me, Ala^7]–AVP analog. The spectra were acquired without isotropic mixing using eight scans per each echo and antiecho data set in each t_1^*/t_1 increment. See Experimental section for other experimental details. The traces were obtained using the (a) earlier published and the newly suggested HSQC–HECADE sequence (b) without and (c) with sensitivity enhancement. The experimentally observed intensity ratio is very close to 1:2:4, which is expected theoretically.

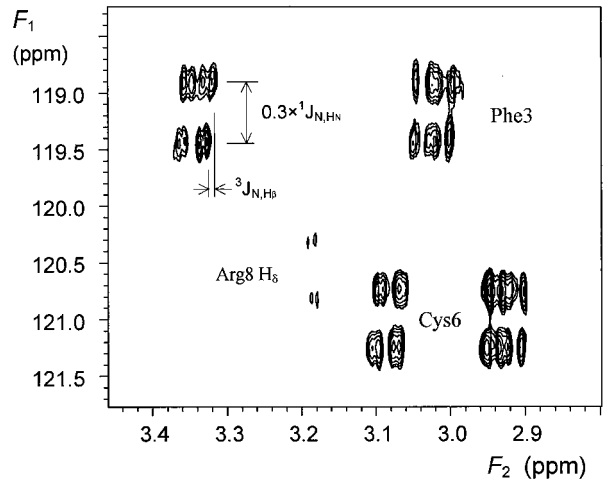

FIG. 4. Expansion of the Phe3 and Cys6 H_β region of the [Me, Ala^7]–AVP analog HSQC-HECADE spectrum marked in Fig. 3b, revealing tilts due to long-range ^{15}N–^1H coupling constants. The coupling-constant values could be evaluated from peak-position differences in F_2 cross sections through the doublet components for each signal.

sensitivity enhancement and I-spin isotropic mixing. The obtaining coupling constants are summarized in Table 1. The solution contains two isomers in approximate 4:1 ratio, but contour levels for only the major isomer are plotted. HECADE spectra from experiments with I-spin isotropic mixing are analogous to (ω_1) X-half-filtered TOCSY spectra (HETLOC) (*8, 9*) but, in addition, I-spin broadband homonuclear decoupling and S-spin chemical-shift labeling in the F_1 domain is achieved. Moreover, the apparent $^1J_{IS}$ splittings in the F_1 domain are largely under experimental control, thus allowing optimization of the required number of t_1 increments and resolution along the F_1 dimension. The coupling constants can be evaluated from F_2 traces through the separated doublet components. The main drawback of the HECADE sequences is the necessity of an additional incremented period for the evolution of heteronuclear couplings. Although this period, labeled t_1^* in Fig. 1, might be significantly shorter than t_1 and the isotropic mixing time, it could still lead to a reduced signal intensity in the case of fast transverse I-spin relaxation. The observed splittings, and consequently directly obtained coupling magnitudes, might be affected by the cross-correlation between dipolar and chemical shift anisotropy relaxation mechanisms and by the scalar relaxation of the second kind (*10, 11*), resulting, respectively, in different relaxation rates of the multiplet components and faster relaxation of the antiphase terms. However, these effects are expected to be of minor importance for the molecules studied, whereas for larger molecules corrections might be necessary (*12*). Another recently proposed family of experiments based on spin-state-selective excitation (S^{3}E) (*13–18*), avoids the t_1^* period. However, since it requires the acquisition of two separate data sets with complementary doublet components it doubles the experiment time to achieve equivalent signal to noise ratio regardless of relaxation. Additionally, whereas a violation of the assumption of uniform $^1J_{IS}$ magnitudes, which is implicit in both experiments, only affects the overall sensitivity in case of the HECADE experiment it leads to incomplete suppression of one of

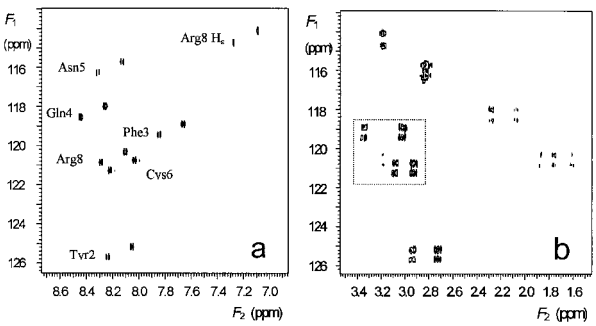

FIG. 3. Expanded (a) amide and (b) H_β proton regions from the ^1H,^{15}N-HSQC–HECADE spectrum of the [Me, Ala^7]–AVP analog at natural isotope abundance. Contour levels for the major isomer only are shown. The spectrum was acquired with a 25-mM 9/1 H_2O/D_2O solution. The region marked by the dotted box is expanded in Fig. 4.

TABLE 1

$^3J_{N,H\beta}$ and $^1J_{N,HN}$ Coupling Constants of the Major Isomer of the [Me, Ala^7]–AVP Analog in [Hz], Obtained by the HSQC–HECADE Experiment

	Tyr2	Phe3	Gln4	Asn5	Cys6	Arg8	Gly9
$^3J_{N,H\beta}{}^a$	−3.3	−3.8	−2.7	−2.4	−3.7	−4.0	—
$^3J_{N,H\beta}$	−1.9	−1.8			−2.1	−2.8	—
$^1J_{N,HN}$	−92.4	−92.7	−92.7	−93.1	−93.6	−92.9	−94.3

Note. The accuracy of coupling constant magnitudes is limited by the F_1 digital resolution and in the present case is estimated to be ca. 0.15 Hz. The $^2J_{N,H\alpha}$ coupling values are partially obscured by H_2O resonance "t_1 noise" and are not included.

[a] Downfield H_β proton signal.

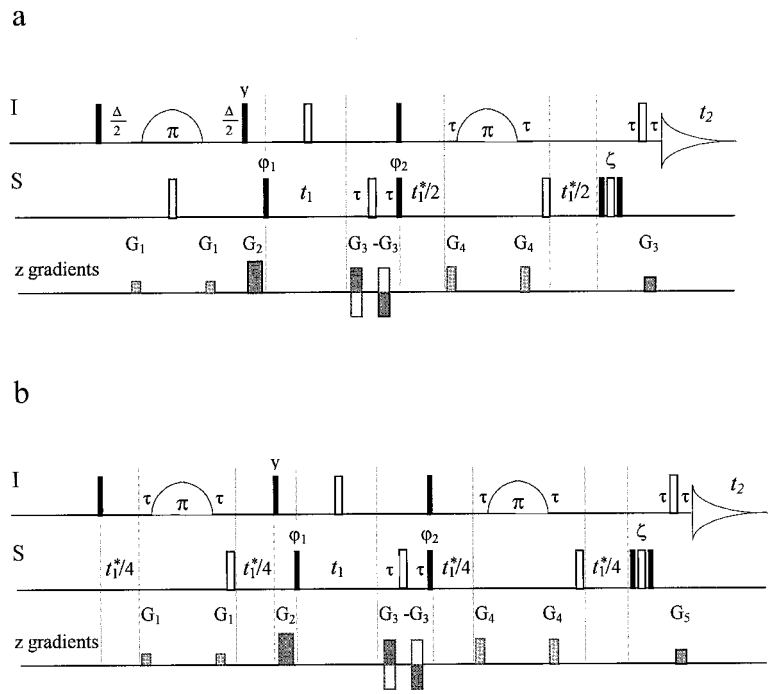

FIG. 5. Pulse sequences for the long-range HSQC–HECADE experiment. Dark-filled and open bars represent $\pi/2$ and π pulses, respectively. All pulses are applied along the rotating-frame x axis unless indicated differently. τ includes the rectangular-shape gradient pulse and a 100-μs recovery time. Gradient pulses G_1, G_2, and G_4 are optional. In the presented application, 1-ms G_1 and G_4 pulses were used with an amplitude of 3 and 4 G/cm respectively, but G_2 was omitted. For ^{1}H–^{13}C experiments gradients G_3 and G_5 with equal duration of 1 ms, and an amplitude of $\pm$10 and 5 G/cm, respectively, were used for echo–antiecho selection, depending on the sign of G_3. The basic phase cycle is the same as for the sequence 1a. (a) "normal" sequence which requires the delay Δ tuned to $0.5/{}^nJ_{IS}$ to obtain maximum transfer amplitude, (b) new experiment with the heteronuclear coupling evolution split into two periods.

the doublet components in case of the S^{3}E sequences. This set of methods has recently found great utility for the measurement of dipolar couplings in partially oriented ^{15}N-enriched proteins. Due to fast transverse relaxation in this application, the measurement of two separate data sets proves still advantageous.

The pulse sequence schemes for the improved long-range versions of the HSQC–HECADE experiment are depicted in Fig. 5. The sequence 5a differs from the one-bond version of 1a by omission of the sensitivity-enhancement elements and the necessary use of selective refocusing pulses applied to I-nuclei (without mutual couplings) to refocus the homonuclear I-spin coupling evolution. Although this sequence is designed to measure active heteronuclear long-range couplings, it is still possible to apply additional I-spin homonuclear polarization transfer using a isotropic TOCSY mixing. In contrast to the rather uniform magnitudes of $^1J_{IS}$ coupling constants the spread of long-range coupling-constant values is usually significant. Consequently, the polarization-transfer-amplitude factor of $\sin(\pi J\Delta)$ might be too small for signal detection in the case of a Δ delay mismatch. This problem is solved in sequence 5b by splitting the t_1^* evolution period into two halves and substituting the constant Δ by an incremented $t_1^*/2$ delay. The resulting spectra reveal an additional antiphase modulation by $\sin(0.5*\pi J t_1^*)$; however, this sequence produces more uniform signal amplitude for all possible J_{IS} magnitudes as long as the maximum t_1^* is long enough. The expected cross-peak patterns for sequences 5a and 5b are drawn in Schemes 2a and 2b, respectively. The comparison of selected cross-peaks obtained in H(2), H(6)-selective experiment applied to a 0.1 M $CDCl_3$ geraniol solution is shown in Fig. 6. Note that method 5b allowed the observation of an additional H(2)–C(3) correlation peak with an active ^2J coupling constant of 0.7 Hz, that was not detected in experiment 5a with Δ tuned to 7 Hz. The heteronuclear long-range coupling constants could also be measured quantitatively by application of I-spin selective HSQC sequence acquired with different Δ delays in the first

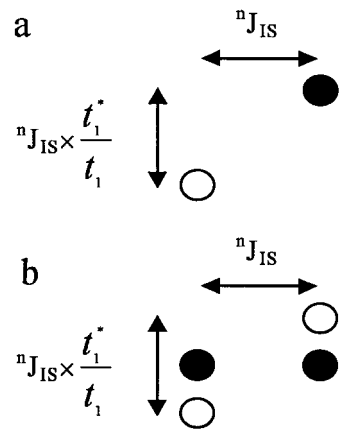

SCHEME 2

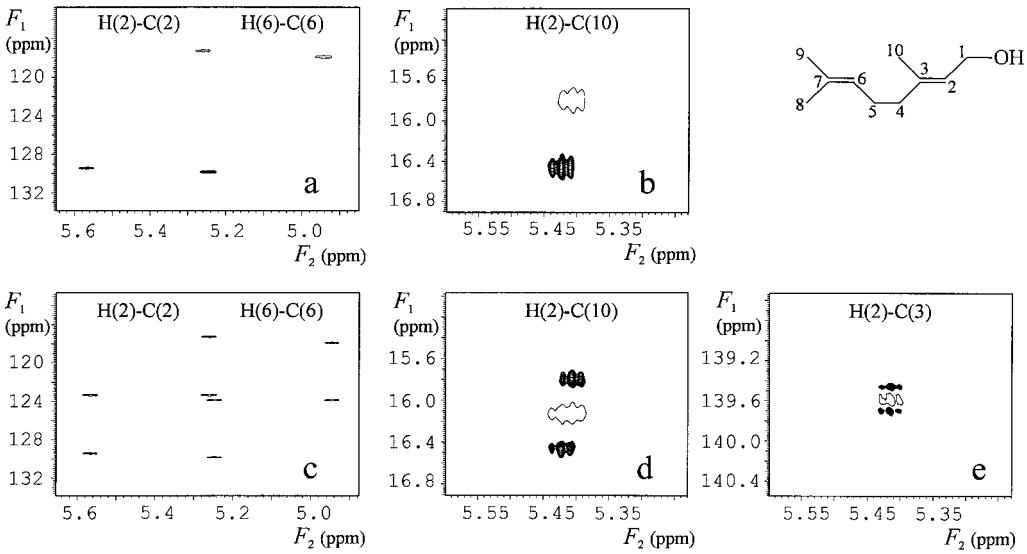

FIG. 6. Expansion of selected cross peaks from the H(2), H(6)-proton selective long-range $^{1}H,^{13}C$-HSQC–HECADE spectra of a 0.1-M geraniol solution in $CDCl_3$ at natural isotope abundance. Spectra were acquired by the methods shown in Fig. 5a (regions (a) and (b)) and in Fig. 5b (regions (c), (d), and (e)), respectively. The one-bond correlation peaks are shown in (a) and (c), $^{1}J_{H(2)-C(2)}$ and $^{1}J_{H(6)-C(6)}$ are equal to 153.4 and 150.6 Hz, respectively. The three-bond correlation signal H(2)–C(10) is shown in (b) and (d), $^{3}J_{H(2)-C(10)} = 8.3$ Hz. The H(2)–C(3) correlation signal in (e) was only obtained with sequence 5b, $^{2}J_{H(2)-C(3)} = 0.7$ Hz. The accuracy of reported coupling constants is estimated from the digital resolution to ca. 0.1 Hz.

INEPT step, and fitting the resulting cross-peak volumes to the function $V(\Delta) = V_0 \sin(\pi J \Delta)\exp(-\Delta/T_2)$ (*19*). However, while this approach offers superior accuracy of the couplings measured, a rather large number of spectra with appropriate signal to noise ratio must be collected for a good fit, which will significantly increase the experimental time, especially for samples at natural isotope abundance.

EXPERIMENTAL

All spectra presented were acquired at 300 K on a Varian Unity Plus 500 spectrometer equipped with a Performa I z-PFG unit and a standard 5-mm ID_PFG probehead (8, 12, and 26 μs high power ^{1}H, ^{13}C, and ^{15}N $\pi/2$ pulses, respectively, were employed). In one-bond transfer HSQC–HECADE experiments a 25-mM solution of the N-methylated, in Ala7 residue, arginine–vasopressin analog ([Me, Ala^{7}]–AVP) in 9/1 H_2O/D_2O was used. Two hundred fifty-six scans were coherently added for each data set for 96 t_1^*/t_1 increments. The maximum t_1, t_1^*, and t_2 times were 64, 19.2, and 652 ms, respectively. A relaxation delay of 1.0 s was used. The delay Δ was tuned to a coupling of 90 Hz. The data matrix containing 96 $\times$ 3200 complex points in t_1 and t_2, was zero-filled to 512 $\times$ 16384 complex points. Cosine and exponential line broadening of 1 Hz functions were applied prior to Fourier transformation in t_1 and t_2, respectively. The DIPSI-2 (*20*) isotropic mixing scheme was applied with ($\gamma B_1/2\pi$ = 7 kHz) for 85 ms to induce magnetization transfer between coupled I-spins. The refocusing of H_N-protons chemical-shift and homonuclear coupling evolution at the center of the t_1^* period was accomplished by a 1.6-ms r-SNOB pulse (*21*) flanked by 1-ms 4 G/cm gradients.

For the selective long-range HSQC–HECADE experiments with the sequences of Figs. 5a and 5b a 0.1-M $CDCl_3$ solution of geraniol was used. In both cases, four scans were coherently added for each data set for 1000 t_1^*/t_1 increments. The maximum t_1, t_1^*, and t_2 times were 50.0 ms, 500.0 ms, and 1.024 s, respectively. A relaxation delay of 1.5 s was used. For the sequence 5a the delay Δ was tuned to a coupling of 7 Hz. The data matrix containing 500 $\times$ 512 complex points in t_1 and t_2, was zero-filled to 2048 $\times$ 2048 complex points. Exponential line broadening of 0.5 Hz was applied prior to Fourier transformation in t_2. Cosine and sine weighting was used in the t_1^*/t_1 domain for the spectra acquired by sequences 5a and 5b, respectively. The refocusing of I-spin chemical-shift and homonuclear coupling evolution at the center of the t_1^* periods was accomplished by a 12.2-ms RE-BURP (*22*) pulse.

CONCLUSIONS

In conclusion, the substantially improved sensitivity, the time-efficient data acquisition, the cleanliness of the spectra, the straightforward data evaluation, the unsurpassed flexibility of the Accordion/ASSCI (*1*) approach, the reduction of line-broadening effects on the coupling-constant evaluation, and the now simpler implementation on commercial spectrometers all contribute to make the HECADE experiment an attractive and highly competitive method for the measurement of heteronuclear coupling constants. The long-range version of the experiment that does not depend on prior knowledge of the coupling-constant magnitude should prove helpful in cases where the detection of cross-peaks with tuned polarization transfers fails.

ACKNOWLEDGMENTS

W.K. thanks to the Warsaw University for the support by Grant 120-501/68/BW-1453/14/99. We thank J. Wójcik and I. Zhukow of the Institute of Biochemistry and Biophysics, Polish Academy of Sciences, and J. Ciarkowski, Z. Grzonka, and F. Kasprzykowski of the Department of Chemistry, Gdańsk University, for the loan of the [Me, Ala^7]–AVP analog and the ^{1}H NMR signal assignments.

REFERENCES

1. W. Koźmiński and D. Nanz, HECADE: HMQC-and HSQC-based 2D NMR experiments for accurate and sensitive determination of heteronuclear coupling constants from E.COSY-type cross peaks, *J. Magn. Reson.* **124,** 383–392 (1997).
2. W. Koźmiński, S. Bienz, S. Bratovanow, and D. Nanz, Pure-phase homo- and heteronuclear *J* spectra with tilted cross peaks for an accurate determination of coupling constants, *J. Magn. Reson.* **125,** 193–196 (1997).
3. W. Koźmiński, The new active-coupling-pattern tilting experiments for an efficient and accurate determination of homonuclear coupling constants, *J. Magn. Reson.* **134,** 189–193 (1998).
4. A. L. Davis, J. Keeler, E. D. Laue, and D. Moskau, Experiments for recording pure-absorbtion heteronuclear correlation spectra using pulsed field gradients, *J. Magn. Reson.* **98,** 207–216 (1992).
5. L. E. Kay, P. Keifer, and T. Saarinen, Pure absorbtion gradient enhanced heteronuclear single quantum correlation spectroscopy with improved sensitivity, *J. Am. Chem. Soc.* **114,** 10,663–10,665 (1992).
6. J. R. Garbow, D. P. Weitekamp, and A. Pines, Bilinear rotation decoupling of homonuclear scalar interactions, *Chem. Phys. Lett.* **93,** 504–509 (1982).
7. A. Bax, Broadband homonuclear decoupling in heteronuclear shift correlation spectroscopy, *J. Magn. Reson.* **53,** 517–520 (1983).
8. M. Kurz, P. Schmieder, and H. Kessler, HETLOC, eine effiziente Methode zur Bestimmung heteronuclearer Weitbereichskopplungen mit dem Heterokern in natürlicher Häufigkeit, *Angew. Chem.* **103,** 1341–1342 (1991). [*Angew. Chem. Int. Ed. Engl.* **30,** 1329–1330 (1991)]
9. U. Wollborn and D. Leibfritz, Measurement of heteronuclear long-range coupling constants from inverse homonuclear 2D NMR spectra, *J. Magn. Reson.* **98,** 142–146 (1992).
10. A. Abragam, "Principles of Nuclear Magnetism," Clarendon Press, Oxford (1961).
11. A. Rexroth, P. Schmidt, S. Szalma, T. Geppert, H. Schwalbe, and C. Griesinger, New principle for the determination of coupling constants that largely suppresses differential relaxation effects, *J. Am. Chem. Soc.* **117,** 10,389–10,390 (1995).
12. A. Meissner, T. Schulte-Herbrüggen, and O.W. Sørensen, Relaxation artifacts and their suppression in multidimensional E. COSY-type NMR experiments for measurement of J coupling constants in ^{13}C- or ^{15}N-labeled proteins, *J. Am. Chem. Soc.* **120,** 7989–7990 (1998).
13. A. Meissner, J. Ø. Duus, and O. W. Sørensen, Spin-state-selective excitation. Application for E. COSY-type measurement of J_{HH} coupling constants, *J. Magn. Reson.* **128,** 92–97 (1997).
14. M. D. Sørensen, A. Meissner, and O. W. Sørensen, Spin-state-selective coherence transfer via intermediate states of two-spin coherences in IS spin systems: Application to E. COSY-type measurements of J coupling constants, *J. Biomol. NMR* **10,** 181–186 (1997).
15. A. Meissner, T. Schulte-Herbrüggen, and O. W. Sørensen, Spin-state-selective polarization or excitation for simultanous E. COSY-type measurements of ^{3}J(C′, H$^\alpha$) and ^{3}J(H^N, H$^\alpha$) coupling constants with enhanced sensitivity and resolution in multidimensional NMR spectroscopy of ^{13}C,^{15}N-labeled proteins, *J. Am. Chem. Soc.* **120,** 3803–3804 (1998).
16. P. Andersson, K. Nordstrand, M. Sunnerhagen, E. Liepinsch, L. Turovskis, and G. Otting, Heteronuclear correlation experiments for the determination of one-bond coupling constants, *J. Biomol. NMR* **11,** 445–450 (1998).
17. P. Andersson, J. Weigelt, and G. Otting, Spin-state selection filters for the measurement of heteronuclear one-bond coupling constants, *J. Biomol. NMR* **12,** 435–441 (1998).
18. W. Koźmiński, Simplified multiplet pattern HSQC–TOCSY experiment for accurate determination of long-range heteronuclear coupling constants, *J. Magn. Reson.* **137,** 408–412 (1999).
19. A. Bax, K. A. Farley, and G. S. Walker, Increased HMBC sensitivity for correlating poorly resolved proton multiplets to carbon-13 using selective or semi-selective pulses, *J. Magn. Reson. A* **119,** 134–138 (1996).
20. A. J. Shaka, C. J. Lee, and A. Pines, Iterative schemes for bilinear operators: Aplication to spin decoupling, *J. Magn. Reson.* **77,** 274–293 (1988).
21. Ē. Kupče, J. Boyd, and I. D. Campbell, Short selective pulses for biochemical applications, *J. Magn. Reson. B* **106,** 300–303 (1988).
22. H. Geen and R. Freeman, Band-selective radiofrequency pulses, *J. Magn. Reson.* **93,** 93–141 (1991).